

Reconfigurable graphene-based multi-input multi-output antenna design for THz applications

Reem Hikmat Abd, Hussein A. Abdulnabi

Department of Electrical Engineering, College of Engineering, AL-Mustansiriyah University, Baghdad, Iraq

Article Info

Article history:

Received Oct 6, 2022

Revised Oct 19, 2022

Accepted Nov 28, 2022

Keywords:

Graphene
Microstrip
MIMO antenna
Unit cell

ABSTRACT

This paper presents a compact graphene-based multi-input multi-output (MIMO) antenna for wireless communications operating in frequency band (0.1-10) THz. This work has been performed with four ports microstrip antennas based on $37 \times 88 \mu\text{m}^2$, a silicon dioxide (SiO_2) substrate and copper on the ground layer, with high isolation by a series of unit cells of graphene selected between adjacent patches to reduce the transmission coefficient and antenna size. Graphene's chemical potential will change by changing the connected DC voltage, leading to bandwidth and resonant frequency variation. The simulation has a reflection coefficient is less than -10 dB at (4.5-10) THz of the frequency scale, mutual coupling (< -15 dB), and the gain from (4.7-9) THz is (1.6-6.7254) dB. This paper aims to provide wideband, efficient and reconfigurable with simple graphene-based MIMO antenna for THz applications.

This is an open access article under the [CC BY-SA](https://creativecommons.org/licenses/by-sa/4.0/) license.



Corresponding Author:

Reem Hikmat Abd

Department of Electrical Engineering, College of Engineering, AL-Mustansiriyah University
Baghdad, Iraq

Email: reem.engineer89@gmail.com

1. INTRODUCTION

Graphene, a typical 2D material made from graphite, has attracted attention recently due to its unique properties. Applications of graphene include those in the thermal, mechanical, optical, medical, and electrical fields [1]. The antenna's surface conductivity can be tuned by applying an external electrical field to a graphene layer [2]. In addition, since the graphene's resistivity decreases rapidly with increasing electrostatic bias voltage, it is simple to control graphene-based antennas. Based on this property, a reconfigurable antenna with varied radiation patterns [3]. Graphene has greater environmental affinity and chemical stability than traditional metals. Graphene is ideally suited for use as a substitute for metal in the potential applications of future wireless communication systems, including antennas and attenuators [4]. The graphene plasmonic characteristic can make antennas and other devices smaller. Graphene devices, including antennas, absorbers, waveguides, polarizers, and filters, were developed for the optical, microwave, and terahertz regimes [5]. Graphene is utilized to produce high-performance antennas as radiating elements in antennas [6]. Due to the unique properties of graphene, it is also adjustable and exhibits greater radiation efficiency than metallic material [7]. 0.1 to 10 THz of the frequency range offers exceptional opportunities for sophisticated applications like wireless communications that offer data rates of hundreds of gigabits per second or terabits per second [8]. However, Terahertz wireless communication frequency spectrum faces challenges, such as attenuation, high absorptions, path loss and multipath fading [9]. Therefore, the MIMO system is an excellent choice to handle these issues due to its modified chemical potential, improving the wireless communication system's capacity and efficiency [10]. The central technology for 5G communication has been recognized as MIMO technology because it allows systems to reach peak data speeds and improve

spectrum efficiency. Additionally, it provides a sizable capacity improvement over traditional SISO (single-input-single-output) systems. The MIMO antenna system is more resilient to fading channel and noise conditions than a SISO antenna system (for more realistic channel conditions) [11], [12]. Consequently, modern wireless applications necessitate a higher isolation level in compressed MIMO. Mutual coupling of less than -15 dB necessitates having enough spacing between the antennas, which can be calculated as $\lambda/2$ or, for even more excellent isolation, $\lambda/4$ of the frequency used. Reducing the channel capacity loss (CCL), lowering the envelop correlation coefficient (ECC) and increasing diversity gain (DG) can be done by reducing the mutual coupling [13]. Due to the band gap in their frequency response, several unit cells, also known as metamaterial (MTM), are utilized to provide enhanced isolation between adjacent elements. The MTM band gaps have the potential to function as band-notch filters and eliminate the possibility of mutual coupling between adjacent antenna elements [14]. Geyikoğlu *et al.* [15] presented a two-layer graphene monopole antenna designed for operating at 1.65 THz with dimensions $32 \times 65 \mu m^2$ that is used for medical applications (cancer detection and treatment). Research by Rasheed and Abdunabi [9] shows the toothed log-periodic antenna with bandwidth (7-10) THz and return loss is less than -10 dB. Alharbi and Sorathiya [16] show the micro-sized circular patch-shaped Yagi-like MIMO antenna placed on Polyimide substrate $620 \times 800 \mu m^2$ with a dual operating band and a minimum return loss of -26.59 dB. Nickpay *et al.* [17], display a wideband nanoribbon graphene-based antenna with double rectangular rings; the antenna has a minimum return loss of -24dB and average radiation efficiency of approximately 44%. Table 1 presents the comparative analysis of the proposed MIMO antenna with previously published results.

Table 1. Comparative analysis of the proposed design and previously published articles

Reference	Type	Frequency range (THz)	Dimension ($\mu m \times \mu m$)	Gain (dB)	Bandwidth (THz)	Return loss (dB)
[9]	SISO	0.1-10	-	6.1	(7-10)z	< -10
[15]	SISO	-	(32×65)	8.52	(1.64-1.665)	-28.7056
[16]	MIMO	1-30	(620×800)	~7	10.69	-26.59
[17]	SISO	-	-	2.45	-	-24
This work	MIMO	0.1-10	(37×88)	6.725	(4.5 - >10)	-44.563

In this study, we proposed a graphene-based microstrip MIMO antenna with a wideband frequency scale and operating frequency that can be tuned by varying the chemical potential. With good performance, return loss, transmission coefficient, bandwidth, gain and directivity. The paper is summarised in; section 2 shows the conductivity of graphene and the MIMO antenna design; section 3 presents the simulation results and discussion; and in section 4, the results of this research have been discussed.

2. METHOD

2.1. Graphene conductivity

The two-dimensional structure describes graphene with excellent electrical characteristics. The material properties of graphene are dispersive, and their value can be modified by varying the frequency with other variables [18]. Graphene thickness is only one atom. The surface conductivity of single-layer graphene depends on its properties, such as relaxation time, frequency, and chemical potential [19]. The conductivity of Graphene can be described by a surface conductivity that is denoted by $\sigma(\omega, \mu_c, \Gamma, T)$ and which is calculated by using the Drude Forma [20]:

$$\sigma(\omega, \mu_c, \Gamma, T) = \frac{j e^2 (\omega - j 2\gamma)}{\pi \hbar^2} \left[\frac{1}{(\omega - j 2\gamma)^2} \int_0^\infty \epsilon \left(\frac{\partial f_d(\epsilon)}{\partial \epsilon} - \frac{\partial f_d(-\epsilon)}{\partial \epsilon} \right) d\epsilon \int_0^\infty \epsilon \left(\frac{\partial f_d(-\epsilon) - f_d(\epsilon)}{(\omega - j 2\gamma)^2 - 4(\epsilon/\hbar)^2} d\epsilon \right. \right. \quad (1)$$

Where $f_d = (e^{(\epsilon - \mu_c)/k_B T} + 1)^{-1}$, ω is the angular frequency in rad/sec, e is the electron charge, γ is the scattering rate in s^{-1} , \hbar is the reduced planck's constant, k_B is the Boltzmann constant, T is the temperature in Kelvin and μ_c is the chemical potential in eV (which can be controlled by applying a bias voltage or by chemical doping). The Kubo formula is integral [21]. And it's simplified as represented in (2)-(4). The intra-band contribution causes the first term in (2), and the interband contribution causes the second term [22].

$$\sigma = \sigma_{inter} + \sigma_{intra} \quad (2)$$

$$\sigma_{intra}(\omega, T, \mu_c, \gamma) = \frac{e^2 k_B T \tau}{\pi \hbar^2} \left[\frac{\mu_c}{k_B T} + 2 \ln \left(e^{\frac{-\mu_c}{k_B T}} + 1 \right) \right] \frac{1}{\omega - j 2\gamma} \quad (3)$$

$$\sigma_{\text{inter}}(\omega, T, \mu_c, \gamma) = \frac{-je^2}{4\pi h} \ln \left(\frac{2|\mu_c| - (\omega - j2\gamma)h}{2|\mu_c| + (\omega - j2\gamma)h} \right) \quad (4)$$

At 1 THz, the intraband term predominates the graphene conductivity. The intraband conductivity real part is much higher than the imaginary part [23]. Above 1 THz, interband conductivity dominates, even though its real part is significantly lower than its imaginary part. However, both terms are considered when calculating graphene's surface impedance. As shown in the following equation, V_b is the applied voltage [5]:

$$Z_{S=1/\sigma(\omega)} = R_S(V_b) + j X_S(V_b) \quad (5)$$

2.2. Microstrip patch antenna

2.2.1. The rectangular patch antenna

As represented in Figure 1, the width (W) and length (L) of the rectangular patch microstrip antenna dimensions are shown in (6), (7) [24]:

$$W = \frac{c}{2f_r \sqrt{\frac{\epsilon_r + 1}{2}}} \quad (6)$$

$$L = L_{\text{eff}} - 2\Delta L \quad (7)$$

where

$$L_{\text{eff}} = \frac{c}{2f_r \sqrt{\epsilon_{\text{reff}}}} \quad (8)$$

$$\Delta L = 0.412h \frac{(\epsilon_{\text{reff}} + 0.3) \left[\frac{W}{h} + 0.264 \right]}{(\epsilon_{\text{reff}} - 0.258) \left[\frac{W}{h} + 0.8 \right]} \quad (9)$$

Where ΔL the extension length, c is the free-space velocity of the electromagnetic wave (3×10^8 m/s), f_r is the resonant frequency, ϵ_{reff} is the effective dielectric constant of MSPA, h is the thickness of the substrate, and ϵ_r is the dielectric constant.

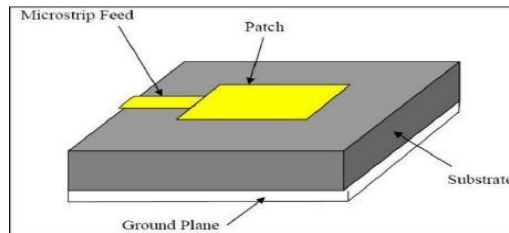


Figure 1. Rectangular microstrip patch antenna

2.2.2. The feed line

The width (W_f) is calculated by adjusting the expected characteristic impedance (Z_c) as in (10) or (11) [25]:

$$Z_c = \frac{60}{\sqrt{\epsilon_r}} \ln \left[\frac{8h}{W_f} + \frac{W_f}{8h} \right] \quad (10)$$

Where $\frac{W_f}{h} \leq 1$ or

$$Z_c = \frac{60}{\sqrt{\epsilon_r}} \ln \left[\frac{8h}{W_f} + \frac{W_f}{8h} \right] \quad (10)$$

Where $\frac{W_f}{h} \geq 1$, moreover, the feed line length (L_f) is shown in (12), (13) [26]:

$$L_f = \frac{1}{4} \lambda_g \quad (12)$$

$$\lambda_g = \frac{c}{f_r \sqrt{\epsilon_r}} \quad (13)$$

Where λ_g is the wavelength

2.2.3. The ground plane

The ground plane of the rectangular microstrip is made from a metallic material, and it functions similarly to a dipole antenna over a ground plane. It contributes to forming a radiation pattern in the forward direction; the fields terminate at the ground from the patch. can be calculated by using (14), (15) [27] :

$$L_g = L \times 2 \tag{14}$$

$$W_g = W \times 2 \tag{15}$$

2.3. Graphene MIMO antenna design

The geometry of the proposed design shown in Figure 2(a) has four patches of graphene thickness of 0.001 nm and a relaxation time of 0.1 ps based on silicon dioxide (SiO_2) substrate with a thickness of $10\mu m$ with $\epsilon_r=3.9$. The ground is made from copper, two-layer above the substrate with a thickness of $1\mu m$ of Alumina and silicon crystalline. The edge-to-edge distance between the radiating elements in the MIMO antenna is maintained at 0.13510λ ($7 \mu m$). Figure 2(b) represents a single-uni cell design. A series of five-unit cells made of graphene, placed between adjacent patches to reduce mutual coupling and MIMO size, is used as a decoupling structure, and the 3D view of the graphene MIMO antenna is represented in Figure 2(c). Table 2 displays the optimal values of all dimensions of a proposed MIMO antenna design.

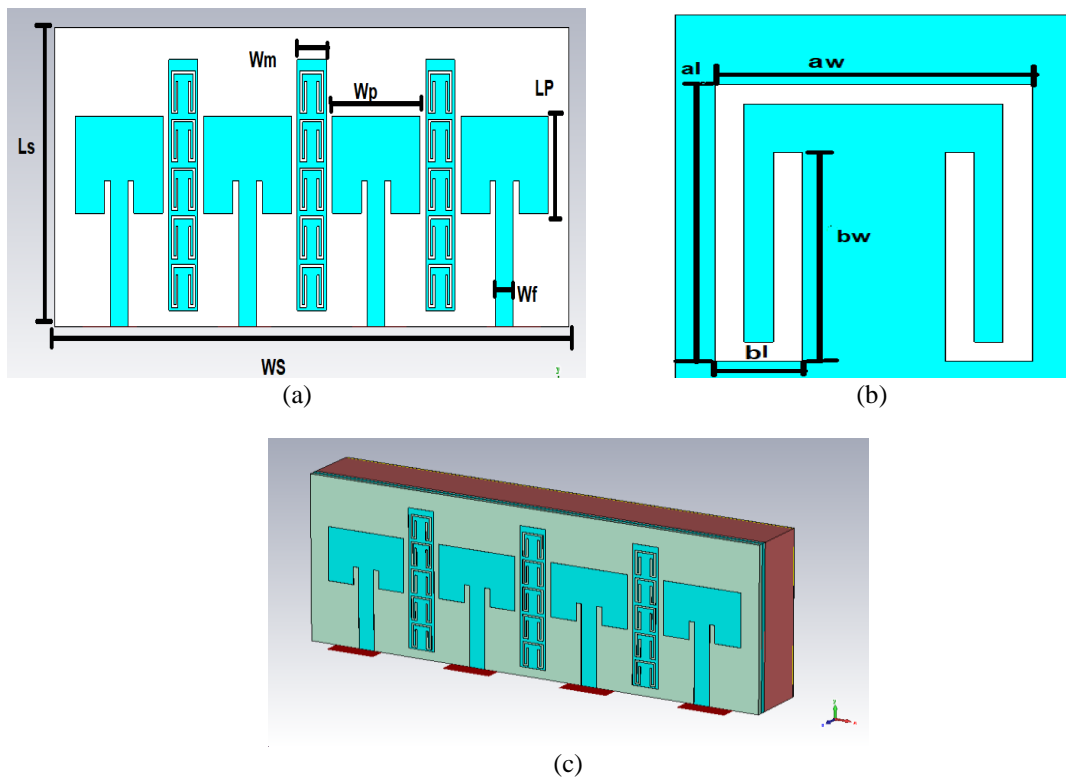


Figure 2. MIMO antenna design (a) front view, (b) zoomed unit cell, and (c) 3D view

Table 2. The dimensions of the microstrip MIMO antenna

Parameters	Value (um)	Parameters	Value (um)
Ws	88	al	5.3
Ls	37	aw	4
Lp	12	wm	5
Wp	15	bl	4
wf	3	bw	1.1

3. RESULTS AND DISCUSSION

Computer simulation technology (CST) Studio version 2020 was used to run graphene-based MIMO antenna simulation. The MTM unit cell used in this design has negative permittivity ϵ_r and negative

permeability μ_r , shown in Figure 3(a), with the S parameter represented in Figure 3(b). The proposed antenna is illustrated for a wide range of chemical potential μ_c values from $\mu_c=0.1\text{eV}$ to 1eV . Bandwidth and resonant frequency are modified with the variation of chemical potential μ_c . Figures 4(a), (b) and 5(a), (b) (in appendix) show the performance of the MIMO antenna with and without metamaterials. The mutual coupling between two radiating elements is diminished by inserting MTM unit cells between every two adjacent patches and reduced by 2 dB. At $\mu_c=1\text{eV}$, the operating bandwidth (4.5-10) THz, with a minimum return loss of -44.563 dB, is present in Figure 5(a) and the transmission coefficient (<-15), shown in Figure 5(b). The gain of the MIMO antenna (1.6-6.725) dB at (4.7-9) THz is illustrated in Figure 6. The operational bandwidth and the mutual coupling at different μ_c values are shown in Figures 7(a), (b) and 8(a), (b) (in appendix). MIMO antenna's radiation patterns at the frequency (5, 10) THz are displayed in Figures 9-10, respectively, showing the antenna's directivity increase by increasing the frequency in the operating band.

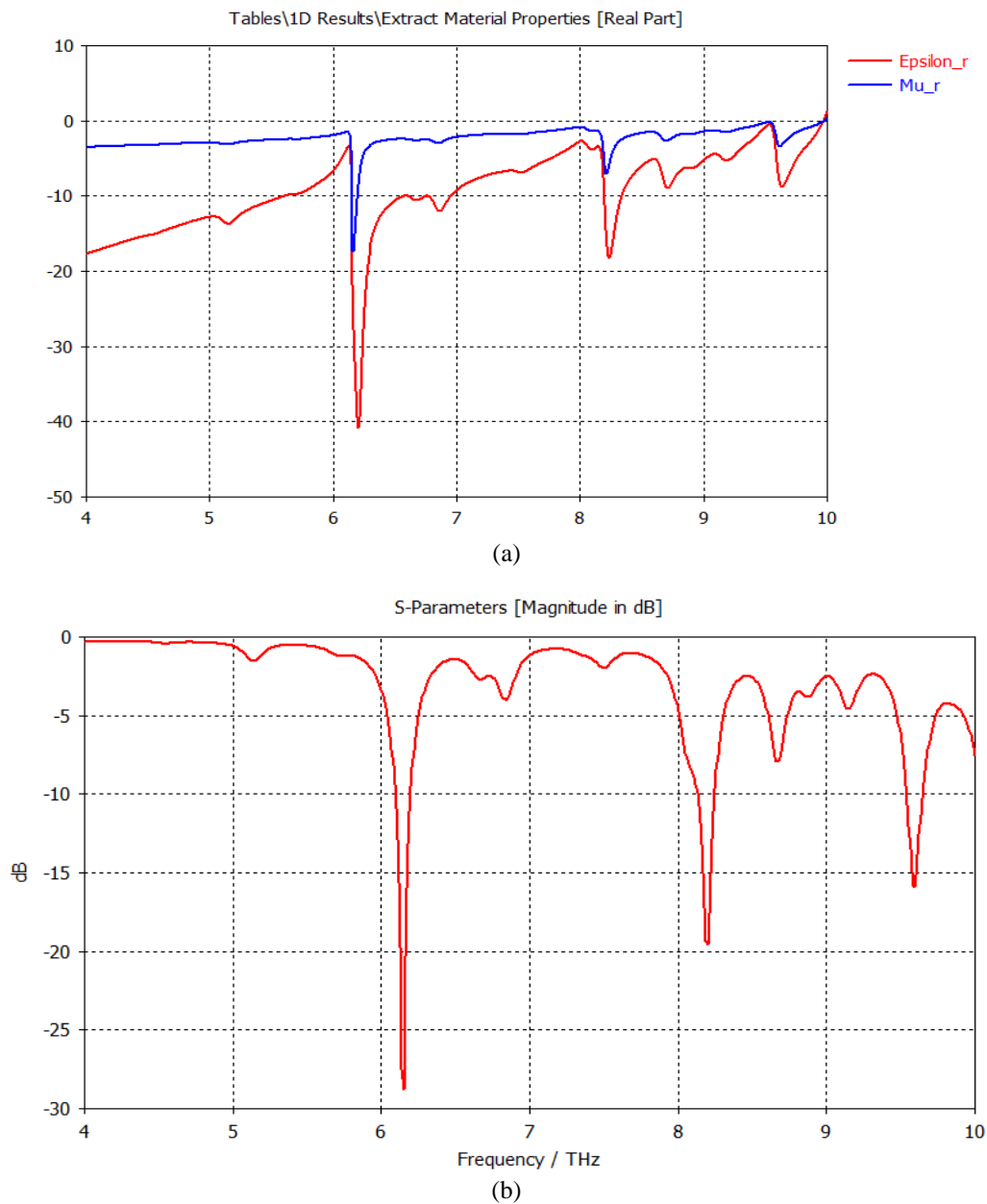


Figure 3. MTM unit cell performance (a) ϵ_r and μ_r parameters and (b) S-parameter

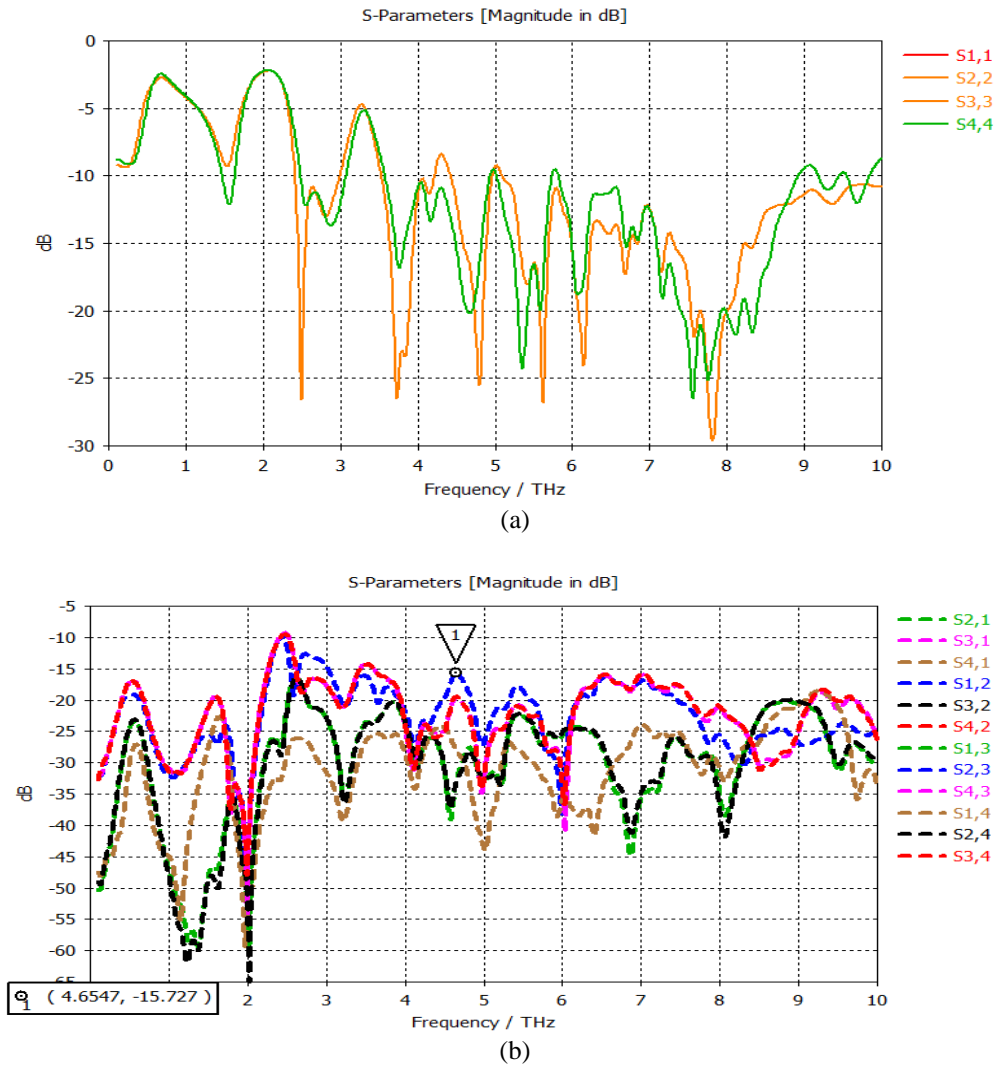


Figure 4. MIMO performance at $\mu_c=1\text{ev}$ without metamaterials (a) reflection coefficient and (b) transmission coefficient

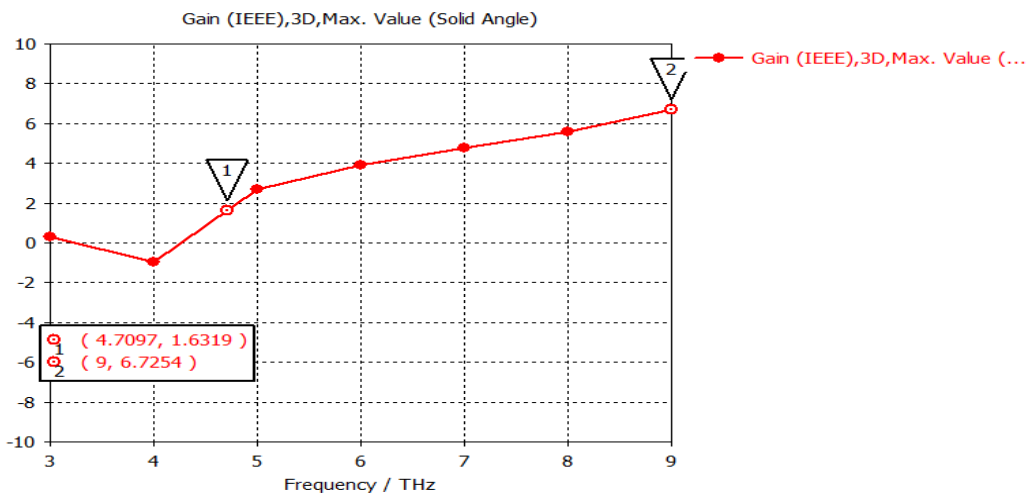


Figure 6. MIMO antenna's gain at $\mu_c=1\text{ev}$

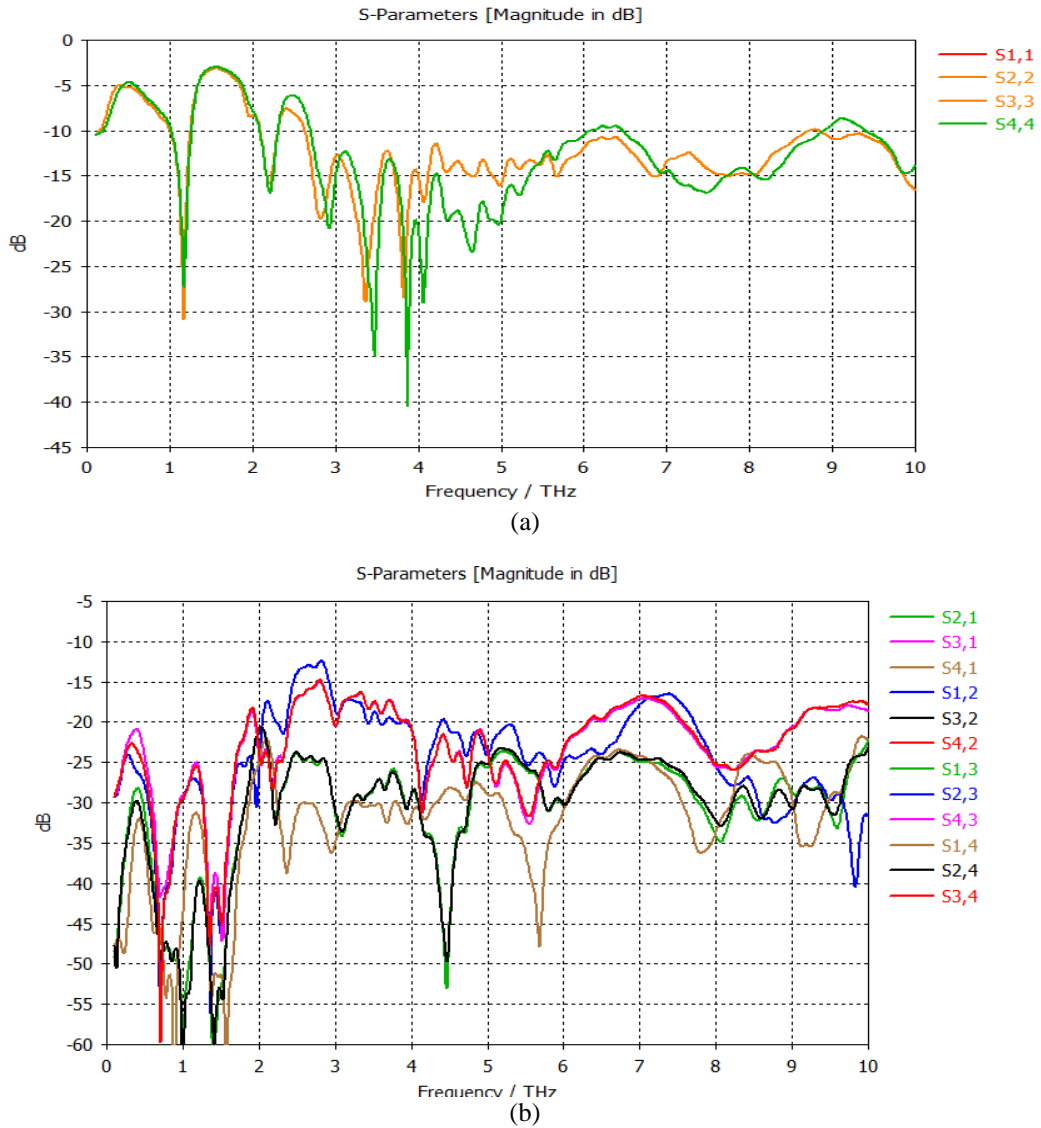


Figure 7. MIMO performance at $\mu c=0.5\text{ev}$ (a) reflection coefficient and (b) transmission coefficient

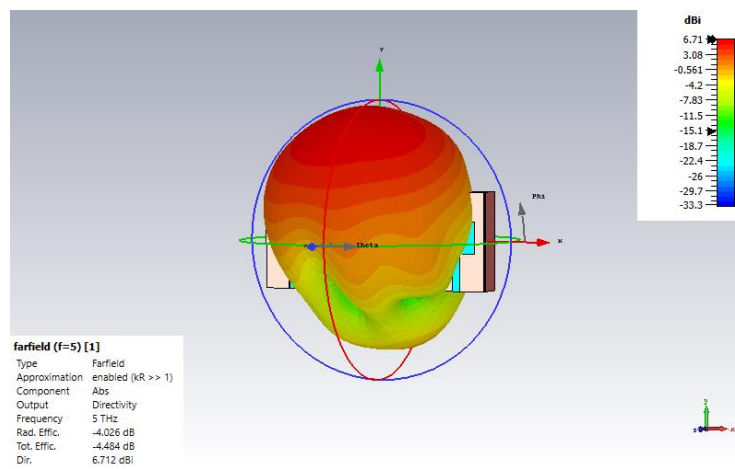


Figure 9. MIMO antenna's radiation pattern at 5 THz

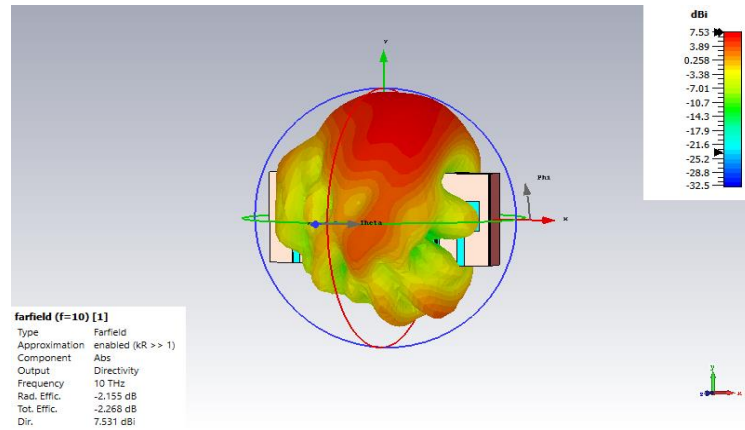


Figure 10. MIMO antenna's radiation pattern at 10 THz

4. CONCLUSION

This paper presents the design, analysis and simulation of a graphene-based MIMO antenna used in THz applications. This design operates at (4.5-10)THz, with a high degree of isolation (<-15) dB. The gain (1.6-6.725) dB with high directivity. The bandwidth, radiation pattern and resonance frequency scale are shifted by adjusting the applied DC voltage, so a reconfigurable MIMO antenna has resulted

APPENDIX

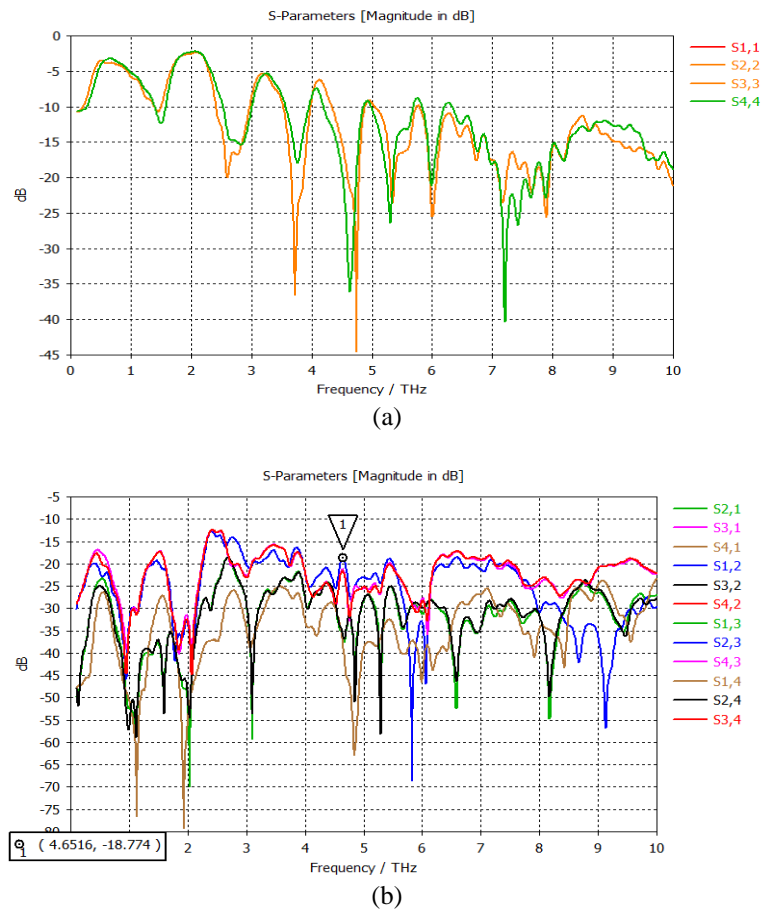


Figure 5. MIMO performance at $\mu_c=1\text{ev}$ with metamaterials (a) reflection coefficient and (b) transmission coefficient

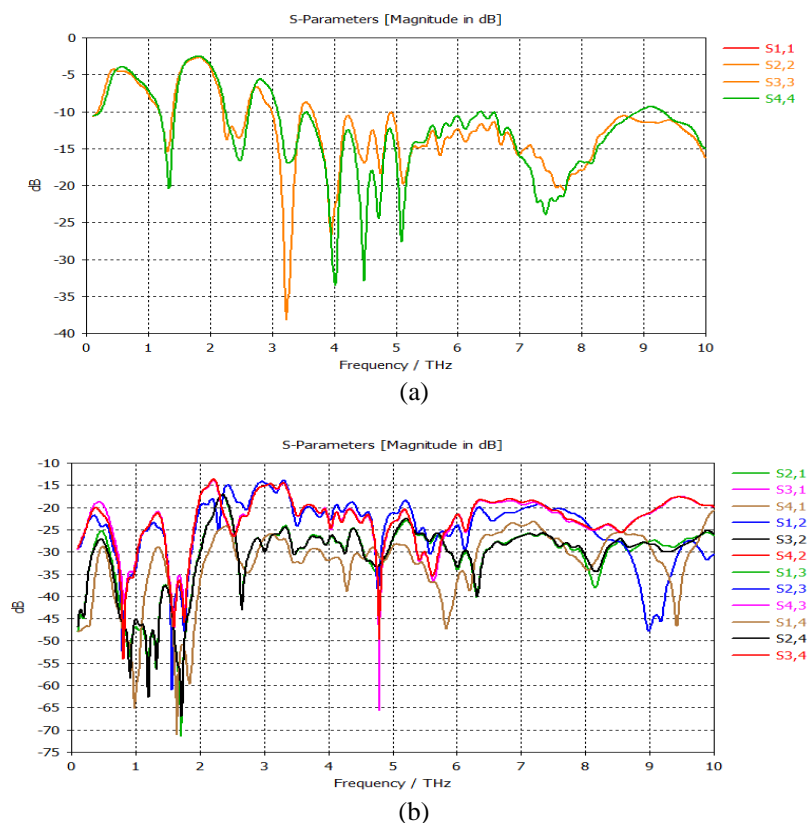


Figure 8. MIMO performance at $\mu c=0.7\text{ev}$ (a) reflection coefficient and (b) transmission coefficient

ACKNOWLEDGEMENTS

The authors want to thank AL-Mustansiriyah University for helping and supporting in completing this study (www.uomustansiriya.edu.iq)





REFERENCES

- [1] G. Varshney, S. Gotra, V. Pandey and R. S. Yaduvanshi, "Proximity-Coupled Two-Port Multi-Input-Multi-Output Graphene Antenna with Pattern Diversity for THz Applications," *Nano Communication Networks*, vol. 21, pp. 100246, sep 2019, doi: 10.1016/j.nancom.2019.05.003.
- [2] H. A. Abdalnabi and Y. Y. Al-Aboosi, "Design of Tunable Multiband Hybrid Graphene Metal Antenna in Microwave Regime," *Indonesian Journal of Electrical Engineering and Computer Science*, vol. 12, no. 3, pp. 401-408, Dec 2018, doi: 10.11591/ijeecs.v12.i3.pp1003-1009.
- [3] Z. Xu, X. Dong and J. Bornemann, "Design of a Reconfigurable MIMO System for THz Communications Based on Graphene Antennas," *IEEE Transactions on Terahertz Science and Technology*, vol. 4, no. 5, pp 609-617, Sep 2014, doi: 10.1109/thz.2014.2331496.
- [4] R. Song, X. Chen, S. Jiang, Z. Hu, T. Liu, D.G. Calatayud, B. Mao and D. He, "A Graphene-Assembled Film Based MIMO Antenna Array with High Isolation for 5G Wireless Communication," *National Natural Science Foundation*, vol. 11, no. 5, pp. 2382, Mar 2021, doi: 10.3390/app11052382.
- [5] K. V. Babu, Sudipta Das, Gaurav Varshney, Gorre Naga Jyothi S, Boddapati Taraka Phani Madhav, "A Micro-Scaled Graphene Based Tree-Shaped Wideband Printed MIMO Antenna For Terahertz Applications," *Journal of Computational Electronics*, vol. 21, no. 1, pp. 289-303, doi: 10.21203/rs.3.rs-839983/v1.
- [6] R. H. Mahdi, H. A. Abdalnabi and A. Alsudani, "plasmonic high gain graphene-based antenna array design for ultra wide band terahertz application," *Bulletin of Electrical Engineering and Informatics*, vol. 11, no. 6, pp. 3322-3328, Dec 2022, doi: 10.11591/eei.v11i6.3673.
- [7] S. Azam, M. A. K. Khan, T. A. Shaem and A. Z. Khan, "graphene based circular patch terahertz antenna using novel substrate materials," *2017 6th International Conference on Informatics, Electronics and Vision & 2017 7th International Symposium in Computational Medical and Health Technology (ICIEV-ISCMT)*, Sep 2017, pp. 1-6, doi: 10.1109/iciev.2017.8338605.
- [8] S. A. Khaleel, E. K. Hamad, N. O. Parchin and M. B. Saleh, "MTM-Inspired Graphene-Based THz MIMO Antenna Configurations Using Characteristic Mode Analysis for 6G/IoT Applications," *Electronics*, vol. 11, no. 14, pp. 2152, Jul 2022, doi: 10.3390/electronics11142152.
- [9] F. M. Rasheed, H. A. Abdalnabi, "Toothed log periodic graphene-based antenna design for THz applications," *Bulletin of Electrical Engineering and Informatics*, vol. 11, no. 6, pp. 3364-3352, Dec 2022, doi: 10.11591/eei.v11i6.4256.
- [10] S. F. A. Rahman, N. A. Salleh, M. S. Z. Abidin, and A. Nawabjan, "Humidity effect on electrical properties of graphene oxide back-to-back Schottky diode," *Telecommunication Computing Electronics and Control*, vol. 17, no. 5, pp. 2427-2433, October 2019, doi: 10.12928/telkomnika.v17i5.12800.





- [11] W. M. Abdulkawi, W. A. Malik, S. U. Rehman, A. Aziz, A. F. A. Sheta and M. A. Alkanhal, "Design of a compact dual-band MIMO antenna system with high-diversity gain performance in both frequency bands," *Micromachines*, vol. 12, no. 4, pp. 383, Apr 2021, doi: 10.3390/mi12040383.
- [12] M. F. Ali, R. K. Singh and R. Bhattacharya, "Reconfigurable graphene-based two port dual-band and MIMO antenna for THz applications," *2020 IEEE Students Conference on Engineering & Systems (SCES)*, Jul 2020, pp. 1-5, doi: 10.1109/sces50439.2020.9236760
- [13] M. N. Naik and H. G. Virani, "A compact four port MIMO antenna for millimeterwave applications," *Bulletin of Electrical Engineering and Informatics*, vol. 11, no. 2, pp. 878-885, Apr 2022, doi: 10.11591/eei.v11i2.3689.
- [14] A. Iqbal, O. A. Saraereh, A. Bouazizi and A. Basir, "Metamaterial-based highly isolated MIMO antenna for portable wireless applications," *Electronics*, vol. 7, no. 10, pp. 267, Oct 2018, doi : 10.3390/electronics7100267.
- [15] M. D. Geyikoğlu, K. Hilal, B. Çavuşoğlu, M. Ertugrul and K. ABBASIAN, "Designing Graphene-Based Antenna for Terahertz Wave Ablation (TWA) System," *Erzincan University Journal of Science and Technology*, vol. 15, no. 2, pp. 507-514, Aug 2022, doi: 10.18185/erzifbed.1014513.
- [16] A. G. Alharbi and V. Sorathiya, "Ultra-Wideband Graphene-Based Micro-Sized Circular Patch-Shaped Yagi-like MIMO Antenna for Terahertz Wireless Communication," *Electronics*, vol. 11, no. 9, pp. 1305, Apr 2022, doi: 10.3390/electronics11091305.
- [17] M.-R. Nickpay, M. Danaie and A. Shahzadi, "Wideband rectangular double-ring nanoribbon graphene-based antenna for terahertz communications", *IETE Journal of Research*, vol. 68, no. 3, pp. 1625-1634, May 2022,doi: 10.1080/03772063.2019.1661801.
- [18] N. Qasem and H. M. Marhoon, "Simulation and optimization of a tuneable rectangular microstrip patch antenna based on hybrid metal-graphene and FSS superstrate for fifth-generation applications," *TELKOMNIKA (Telecommunication Computing Electronics and Control)*, vol. 18, no. 4, pp. 1719-1730, Aug 2020, doi: 10.12928/telkomnika.v18i4.14988.
- [19] X.-S. Rong, Q.-M. Wan, H.-L. Peng, Y.-P. Zhang and J.-F. Mao, "A graphene loaded THz patch antenna with tunable frequency," *2018 IEEE World Symposium on Communication Engineering (WSCE)*, Dec 2018, pp 76-79,doi: 10.1109/wsce.2018.8690534.
- [20] G. W. Hanson, A. B. Yakovlev and A. Mafi, "Excitation of discrete and continuous spectrum for a surface conductivity model of graphene," *Journal of applied physics*, vol. 110, no. 11, pp. 114305, Dec 2011, doi: 10.1063/1.3662883.
- [21] F. M. Rasheed and H. A. Abdalnabi, "Multiband graphene-based Mimo antenna in terahertz antenna regime," *2022 2nd International Conference on Computing and Machine Intelligence (ICMI)*, Apr 2022, doi: 10.1109/icmi5296.2022.9873789.
- [22] M. A. Ismail, K. M. M. Zaini and M. I. Syono, "Graphene field-effect transistor simulation with TCAD on top-gate dielectric influences," *TELKOMNIKA (Telecommunication Computing Electronics and Control)*, vol. 17, no. 4, pp. 1845-1852, Aug 2019, doi: 10.12928/telkomnika.v17i4.12760.
- [23] R. T. Hussein and H. A. Abdalnabi, "Zigzag Edges Toothed Log Periodic Terahertz Antenna Design Based on Graphene Hilbert Curve AMC," *2018 Third Scientific Conference of Electrical Engineering (SCEE)*, 2018, pp.140-143, doi: 10.1109/SCEE.2018.8684111.
- [24] D. Bhalla and K. Bansal, "Design of a rectangular microstrip patch antenna using inset feed technique," *IOSR Journal of Electronics and Communication Engineering*, vol. 7, no.4,pp.08-13, 2013, doi: 10.9790/2834-0740813.
- [25] H. M. Marhoon and N. Qasem, "Simulation and optimization of tuneable microstrip patch antenna for fifth-generation applications based on graphene," *International Journal of Electrical & Computer Engineering (2088-8708)*, vol. 10, no. 5, pp. 5546-5558, Oct 2020, doi: 10.11591/ijece.v10i5.pp5546-5558.
- [26] D. Behera, B. Dwivedy, D. Mishra and S. K. Behera, "Design of a CPW fed compact bow-tie microstrip antenna with versatile frequency tunability," *IET Microwaves, Antennas & Propagation*, vol 12, no.6 , pp 841-849, May 2018,doi:10.1049/iet-map.2017.0421.
- [27] S. D. Sateaa, M. S. Hussein, Z. G. Faisal, A. M. Abood and H. D. Satea, "Design and simulation of dual-band rectangular microstrip patch array antenna for millimeter-wave," *Bulletin of Electrical Engineering and Informatics*, vol. 11, no. 1, pp. 299-309, Feb 2022 doi:10.11591/eei.v11i1.3336.

BIOGRAPHIES OF AUTHORS



Reem Hikmat Abd     received a B.Eng. degree in Information Engineering from AL- Nahrain University Baghdad/Iraq in 2011. She is currently Emp. In Information Technology Department, Ministry of Transportation. She can be contacted at email: reem.engineer89@gmail.com.



Hussein A. Abdalnabi     received a B.Eng. degree in Electrical Engineering from AL-Rasheed College Baghdad/Iraq in 1991, a master's degree in Electronic & Communication Engineering Science from Al-Mustansiriyah University in 2000 and a PhD degree in Communication Engineering from the University of Technology, Iraq in 2017. He is currently an Assoc. Prof. in Electrical Engineering Department/Al-Mustansiriyah University. His current research interests include communication and antenna design. He can be contacted by email: Hussein_ali682@yahoo.com.